1278

SEPTEMBER 1976 PPPL-1278

CONF-761012--22

COUNTERSTREAMING-ION TOKAMAK FUSION REACTORS

BY

D. L. JASSBY, R. M. KULSRUD,
F. W. PERKINS, J. KILLEEN,
K. D. MARX, M. G. McCOY,
A. A. MIRIN, M. E. RENSINK,
AND C. G. TULL

PLASMA PHYSICS LABORATORY

**

PRINCETON UNIVERSITY
PRINCETON, NEW JERSEY

This work was supported by U. S. Energy Research and Development Administration Contract E(11-1)-3073. Reproduction, translation, publication, use and disposal, in whole or in part, by or for the United States Government is permitted.

DISCLAIMER

NOTICE

This report was prepared as an account of work sponsored by the United States Government. Neither the United States nor the United States Energy Research and Development Administration, nor any of their employees, nor any of their contractors, subcontractors, or their employees, makes any warranty, express or implied, or assumes any legal liability or responsibility for the accuracy, completeness or usefulness of any information, apparatus, product or process disclosed, or represents that its use would not infringe privately owned rights.

Printed in the United States of America.

Available from
National Technical Information Service
U. S. Department of Commerce
5285 Port Royal Road
Springfield, Virginia 22151

Price: Printed Copy $ * ; Microfiche $1.45

*Pages	NTIS Selling Price
1-50	$ 4.00
51-150	5.45
151-325	7.60
326-500	10.60
501-1000	13.60

Prepared for
Sixth International Conference on Plasma Physics
and Controlled Nuclear Fusion Research
Berchtesgaden, FRG, 6-13 October 1976

COUNTERSTREAMING-ION TOKAMAK FUSION REACTORS*

D. L. Jassby, R. M. Kulsrud, F. W. Perkins

Plasma Physics Laboratory, Princeton University
Princeton, New Jersey 08540, USA

J. Killeen, K. D. Marx, M. G. McCoy, A. A. Mirin, M. E. Rensink, C. G. Tull

National CTR Computer Center
Lawrence Livermore Laboratory, University of California
Livermore, California 94550, USA

ABSTRACT

Tokamak plasmas fueled and heated by energetic neutral-atom beams are characterized by total ion pressure greatly exceeding the electron pressure. For smaller devices with relatively low injection energy, the largest fusion reactivity of energetic-ion plasmas is obtained when oppositely injected D° and T° beams sustain large densities of counterstreaming deuterons and tritons (CIT mode). In this study steady-state ion velocity distributions for the CIT are calculated with a multi-species Fokker-Planck code, and are found to have sufficient thermal spread so that all infinite-medium velocity-space modes are stable. Quasi-stationary operation seems physically realizable, because the injected beams provide all fueling, and the counterstreaming ions can be made to carry the bulk of the plasma current required for equilibrium; a satisfactory magnetic flux-surface configuration is revealed by a particle simulation code.

Steady-state radial profiles of plasma parameters are determined with a coupled Fokker-Planck/radial transport code that includes charge-exchange effects and particle and heat diffusion of "warm" ions and electrons. With inclusion of realistic charge-exchange loss and a significant warm-ion population, the ideal CIT Q-values are found to be reduced by 60 to 70% for a given $\langle n_e \tau_{Ee} \rangle$. For example, $Q = 1.0$ for $W_{inj} = 80$ keV (D°) and 120 keV (T°), when $\langle n_e \tau_{Ee} \rangle = 8 \times 10^{12}$ cm^{-3}s and $\langle n_{hot}/n_e \rangle \simeq 0.7$. Generally, the total ion pressure is 3 to 5 times the electron pressure, and the warm-ion temperature ~ $2T_e$.

1. INTRODUCTION

With the application of intense neutral-beam injection to tokamak plasmas, it becomes possible to sustain plasmas with $\Pi_i >> 1$, where Π_i is the ratio of total ion energy density to the electron energy density. In smaller devices that permit relatively small beam voltage for good penetration, plasmas with $\Pi_i >> 1$ are especially easy to establish because (1) a substantial fraction — perhaps most — of the injected energy is given up to "warm" (i.e., bulk) ions rather than to electrons; (2) decelerated injected ions constitute a significant fraction of the warm-ion population; (3) the energetic ions themselves hold a large fraction of the plasma energy. Considerations (1) and (2) imply that the warm-ion temperature T_i can exceed the electron temperature T_e, even when the energy confinement times τ_{Ei} and τ_{Ee} are comparable. Indeed, in present high-powered injection experiments with W_b = 15-35 keV, the trend toward $T_i > T_e$, $\Pi_i >> 1$ plasmas is already evident [1].

In tokamaks with only modest $n_e\tau_{Ee}$-values, where beam-induced fusion reactions are important, there are certain advantages in minimizing the warm-ion population n_i: (1) For a given $n_e\tau_{Ee}$ and injection power density P_b, a larger T_e — and therefore longer fast-ion lifetime — can be maintained at smaller n_i/n_e. (2) The energetic-ion population generally has a large fusion reactivity $\langle\sigma v\rangle$, so that significant fusion power multiplication Q is attainable in principle even at low $n_e\tau_{Ee}$ and low T_e. In small devices employing state-of-the-art low-energy beams (W_b = 40-100 keV), $\langle\sigma v\rangle$ is maximized when D° and T° beams are injected oppositely to create and sustain counterstreaming-ion velocity distributions [2-4], as in Fig. 1. In this CIT (counterstreaming-ion torus) mode, the streaming ions can be made to drive the bulk of the plasma current required for equilibrium [4,5]. Inasmuch as the injected beams provide all fueling, steady-state operation is possible in principle.

In this work the term CIT denotes that class of D-T plasmas with $\Pi_i >> 1$, $p_{\parallel} > p_{\perp}$, and where the D and T velocity distributions are shifted oppositely in $v_{\parallel}$. Previous studies have been concerned with velocity distributions in ideal CIT operation [2,4]. Near-ideal CIT distributions can be maintained only by minimizing the recycling of decelerated ions and warm neutrals that leave the hot reacting region. In practice, inevitable influx of cold plasma and neutrals will result in a certain warm-ion population with T_i in the range 1-3 T_e. The present paper reports investigations of the energetics and reactor performance of CIT-type operation when non-ideal effects such as charge-exchange loss and large warm-ion populations are included. The object is to determine realistic operating regimes that would offer Q-values of 1 to 2, which are suitable for near-term tokamak applications such as fissile breeding. Our principal computational tools comprise a numerical multispecies Fokker-Planck analysis coupled with a one-dimensional plasma transport code.

2. ION VELOCITY DISTRIBUTIONS

2.1 Start-Up

At the beginning of a cycle the injected fast atoms are trapped by an Ohmic-heated low-density ($n_e \sim 10^{13}$ cm^{-3}), low temperature ($T_e \sim 1$ keV) tokamak plasma. During injection for several slowing-down times (a period

typically less than 1 s), n_e is built up to the range 4 to 8×10^{13} cm^{-3}, T_e reaches a steady-state value of at least several keV, and the ion population becomes dominated by energetic ions. In the steady state, injected energetic neutrals are trapped by charge-exchange with ions traveling in the same direction, by impact ionization on oppositely traveling ions, and by electron ionization. The electron temperature is maintained by Coulomb power deposition from the energetic ions (and by charged fusion-reaction products), Ohmic heating generally being negligible for $\langle T_e \rangle \gtrsim 3$ keV.

2.2 Ideal CIT Performance

The hot-ion velocity distribution functions $f_h(v)$ are calculated with a time-dependent, multispecies, two-velocity-dimensional Fokker-Planck (FP) code [6]. The time derivative of the distribution function for each ion species is written as the sum of a Fokker-Planck collision term, a source term, a charge-exchange loss term, and a term expressing finite particle and energy confinement times. Coulomb interactions (drag, angular scattering, energy diffusion) among all plasma species are included, but the electron distribution is kept Maxwellian.

Initial calculations [2] employed the following ideal conditions: (1) The energetic ions are assumed to be perfectly confined until they decelerate to an energy $2T_e$. (2) Ions with energy $W < 2T_e$ are assumed to be lost at a rate $\tau_p^{-1} \simeq 2\tau_{Ee}^{-1}$. (3) The injected beams provide the only source of particles and heat, so that both T_e and n_e are determined by τ_{Ee} and the ion source strength S. Figure 1 shows the steady-state $f_h(v)$ when the injection energies are W_b = 60 keV (D°), 40 keV (T°), and $n_e\tau_{Ee}$ is of sufficient magnitude to give T_e = 6.0 keV [2]. The dominant Coulomb interaction occurs among ions injected in the same direction, so that f_h for each species resembles a shifted Maxwellian. The hot-ion "temperature" is about 14 keV, with $T_\perp$ slightly greater than $T_\parallel$ because of angular scattering by the long-range Coulomb interaction between counterstreaming ions.

The fusion power gain Q is calculated by integrating reactivity over the D and T velocity distributions, and dividing by the injection power. Figure 2 shows T_e and Q as a function of $n_e\tau_{Ee}$ for various W_b, when fusion alpha particles are not confined. "Break-even" (Q = 1) is attained at $n_e\tau_{Ee} \simeq 2\times10^{12}$ $cm^{-3}s$ and T_e = 3.5 keV. The required fast-ion confinement time is $\tau_h/\tau_{Ee} \simeq (\bar{W}_b - 3/2\ T_e)/1.5\ T_e \gg 1$. It has been shown that, approximately, $T_e \propto (n_e\tau_{Ee})^{2/5}$ and $Q \propto (n_e\tau_{Ee})^{3/5}$ [4].

2.3 Effect of Warm-Ion Population

Although the FP code itself has no explicit spatial treatment, both the finite spatial diffusion time of warm ions and a possible cold-ion influx can be modelled by varying τ_p/τ_{Ee}, where the particle confinement time $\tau_p(v) = [\tau_{min} + (M_h v^2/3T_e)^5]$. (In the following, τ_p denotes τ_{min}.) In these calculations we use $W_{T°} = 3/2\ W_{D°}$, $S_D = 6.5\times10^{13}$ $cm^{-3}s^{-1}$, and a specified τ_{Ee}. Generally, S_T/S_D is adjusted to give $n_T = n_e$. Then both n_e and T_e are determined in part by S_D and τ_{Ee}, but also by τ_p/τ_{Ee}, which determines the build-up of warm-ion population.

(The injected beams have angular profiles of the form $\exp[-b(\cos\theta - \cos\theta_o)^2]$, where θ_o is the direction of injection with respect to the magnetic axis. In our calculations with θ_o = [0° (D°), 180° (T°)], we use

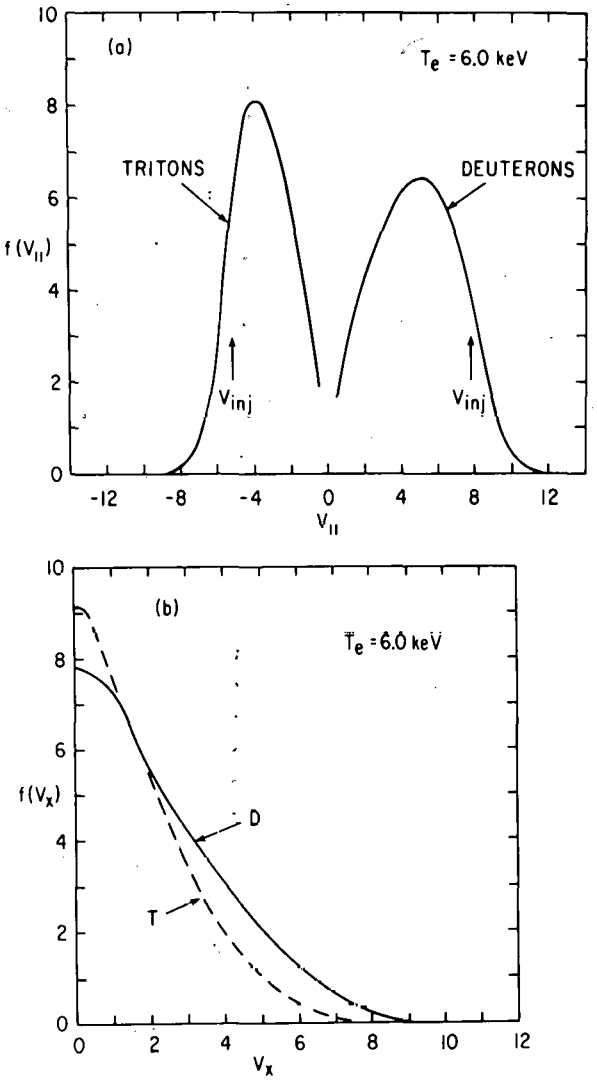

753365

FIG. 1. Steady-state ion velocity distribution in an ideal CIT plasma, (a) parallel and (b) in a direction perpendicular to the magnetic field. Beam injection at W_b = 60 keV (D°), 40 keV (T°), indicated by v_{inj}.

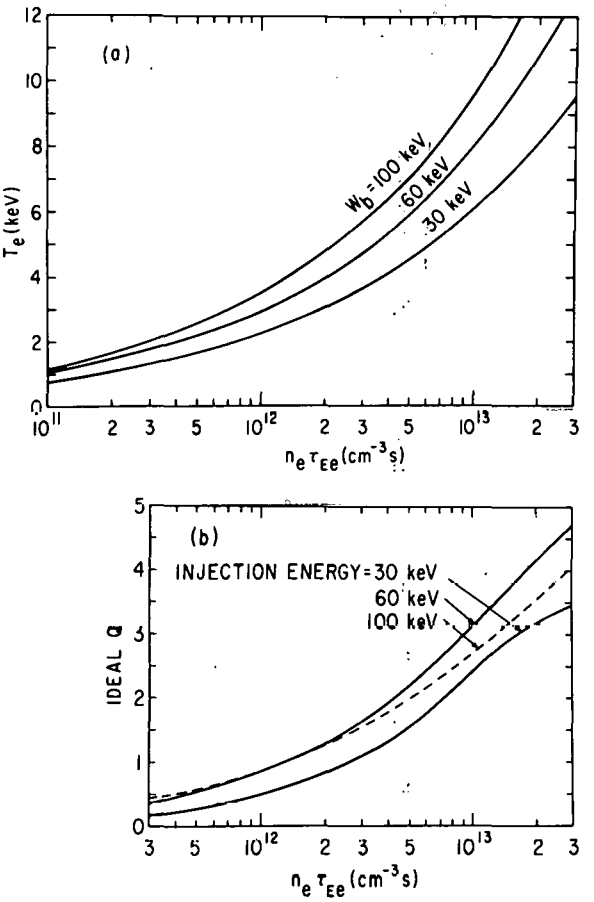

763787

FIG. 2. Dependence of (a) T_e and (b) ideal Q on electron energy confinement parameter for steady-state CIT operation. D° and T° injected at same energy. 17.6 MeV per reaction. Neither charge-exchange loss nor fusion-alpha heating is included.

a width $\Delta\theta = 20°$ (b = 275), but we find that Q is reduced by at most 5% for $\Delta\theta$ up to 80° when W_b = 60 keV (D°). At larger values of W_b, where head-on nuclear collisions are less favorable, oblique injection may be satisfactory.)

Figure 3 shows that both Π_i and $p_\parallel/p_\perp$ decrease significantly with τ_p/τ_{Ee}. The decrease in $p_\parallel/p_\perp$ is due to the nearly isotropic warm-ion population, and to the increased angular scattering of the hot ions by the warm ions. Calculations with D° beam injection alone give $p_\parallel/p_\perp = 3.1$ at $\tau_p/\tau_{Ee} = 1.0$ [see Fig. 4(a)]; thus the value $p_\parallel/p_\perp \simeq 1.9$ obtained with D and T counter-injection at $\tau_p/\tau_{Ee} = 0$ reveals the long-range angular scattering interaction between counterstreaming ions. In the low-$n_e\tau_E$ case, Q is maximum for $\tau_p/\tau_{Ee} \simeq 0.3$. In the high-$n_e\tau_E$ case with 100-keV beams, both beam-target reactions and thermonuclear reactions among warm ions are important, so that maximum Q is achieved at $\tau_p/\tau_{Ee} \simeq 1$-2.5.

With increasing $n_e\tau_{Ee}$, T_e increases and electron drag decreases, so that ions in the counterstreaming distributions are increasingly able to thermalize with each other before slowing down. Then $f_h(v)$ becomes more nearly isotropic, as shown in Fig. 4(b) for W_b = 60 keV, T_e = 12 keV, $\tau_p = \tau_{Ee}$. With sufficiently large $n_e\tau_E$, the CIT evolves into beam-driven thermonuclear operation [7].

2.4 Charge-Exchange Loss

Figure 5 shows the variation of ion parameters and Q with neutral density n_n, for constant S_D and τ_{Ee}. The present model assumes that all fast neutrals formed by charge-exchange are immediately lost from the plasma. For plasmas of practical size, however, the majority of the fast neutrals are re-trapped and eventually ionized, so that n_n would be a factor of 5 to 10 larger than the values listed in Fig. 5 to give the same plasma parameters. The present calculation — unlike that of Sect. 5 — assumes also that warm ions formed from charge exchange leave the plasma immediately. Then charge-exchange loss causes depletion of the lower velocity part of $f_h(v)$, so that $\bar{E}_D$ and Π_i increase significantly with n_n.

2.5 Impurity Ions

The principal effects of an impurity-ion population are to enhance the angular scattering rate of fast ions (proportional to $Z_{eff} = \Sigma n_i Z_i^2/n_e$), and to deplete the reacting-ion population for a given total plasma pressure. In small quantities the impurity ions have the beneficial effect of permitting the streaming ions to drive a large plasma current [8]. The net beam-induced current density is [5,8]

$$J_b = e[n_D\langle V_\parallel\rangle_D + n_T\langle V_\parallel\rangle_T]\left(1 - \frac{1}{Z_{eff}}\right) . \qquad (1)$$

In the present calculations, S_T/S_D is adjusted to give $n_D \simeq n_T$, rather than to maximize J_b. Even in this case the average triton momentum tends to exceed the average deuteron momentum, resulting in significant values of J_b, as shown in Fig. 6(a). Evidently, maximum J_b is reached at $Z_{eff} \simeq 1.5$; at larger Z_{eff}, enhanced isotropization of ion momentum outweighs the increase in $(1 - 1/Z_{eff})$. Figure 6(b) shows that with iron impurity, the reduction in Q is quite tolerable at $Z_{eff} = 1.5$. By increasing the ratio S_T/S_D, it seems feasible to raise J_b to 100 A/cm^2 while keeping n_T/n_D no larger than 2.

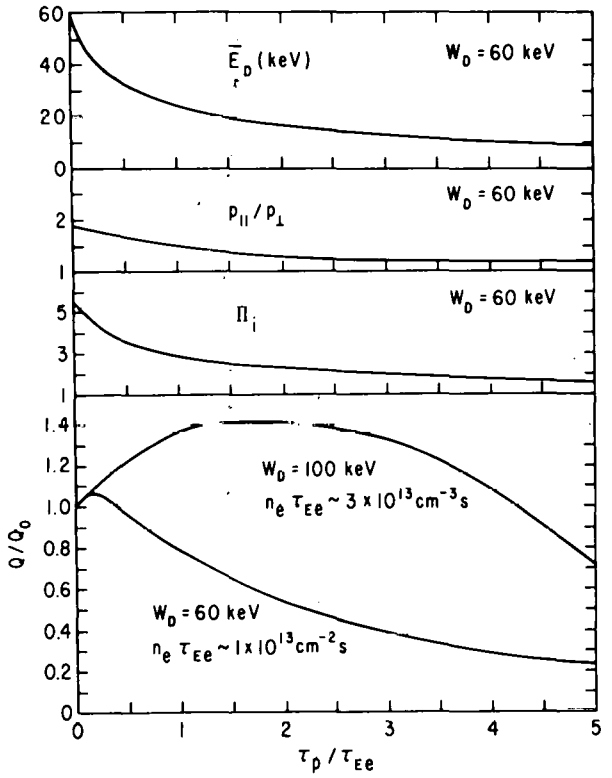

763778

FIG. 3. Effect of warm-ion lifetime τ_p on CIT performance with beam injection at 60 keV (D°), 90 keV (T°). $\bar{E}_D$ = mean deuteron energy, including warm ions. $p_{\parallel}/p_{\perp}$ and Π_i refer to entire ion population. No charge exchange.

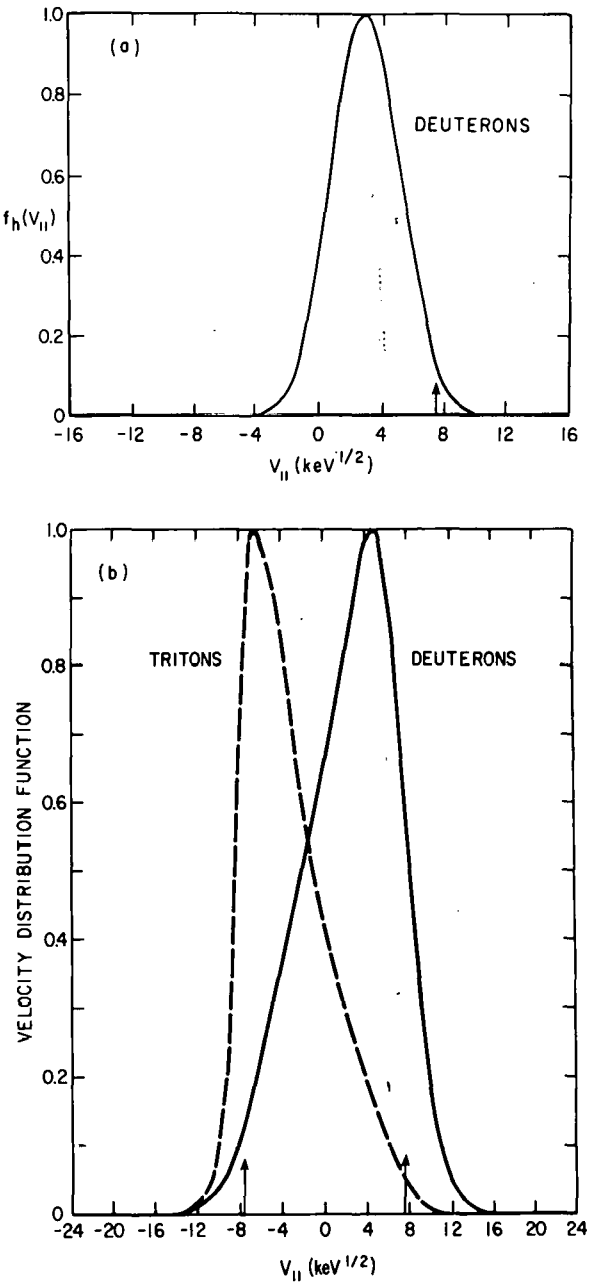

763818

FIG. 4. (a) Steady-state $f_h(v_{\parallel})$ for D° injection at 60 keV. (No counter-injected beam.) T_e = 6.7 keV, $\tau_p = \tau_{Ee}$, $p_{\parallel} = 3.1\, p_{\perp}$, $n_n = 0$. (b) Steady-state $f_h(v_{\parallel})$ for injection at 60 keV (D°), 90 keV (T°), T_e = 12 keV, $\tau_p = \tau_{Ee}$, $n_n = 10^7$ cm^{-3}. Arrows indicate injection velocities.

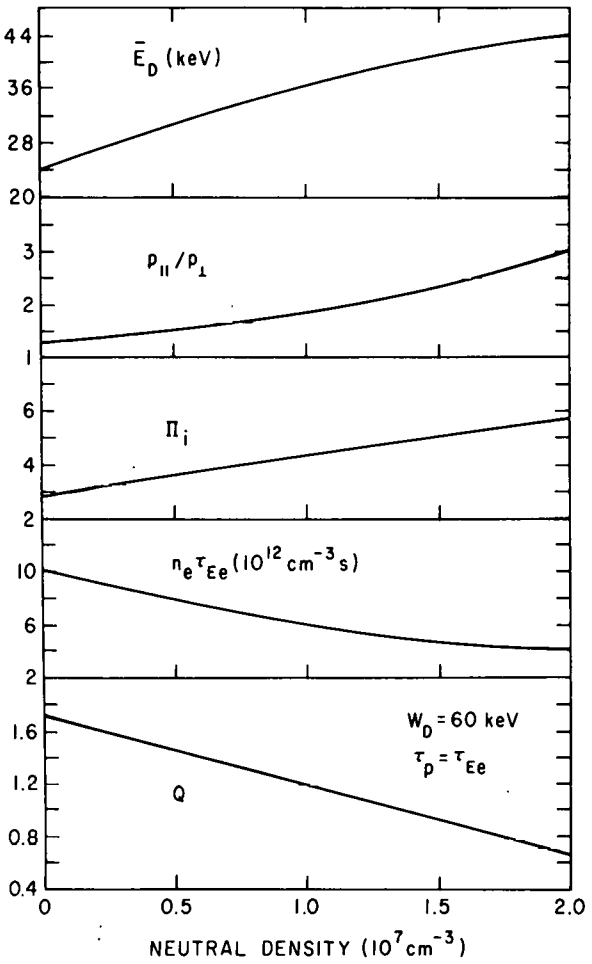

763779

FIG. 5. Effect of neutral density on CIT performance with beam injection at 60 keV (D°), 90 keV (T°). $P_{D°}$ = 0.67 W/cm^3, $\tau_p = \tau_{Ee}$. Fast neutrals and warm ions resulting from charge-exchange are immediately lost from the plasma. $p_{\parallel}/p_{\perp}$ and Π_i refer to entire ion population. 17.6 MeV per reaction.

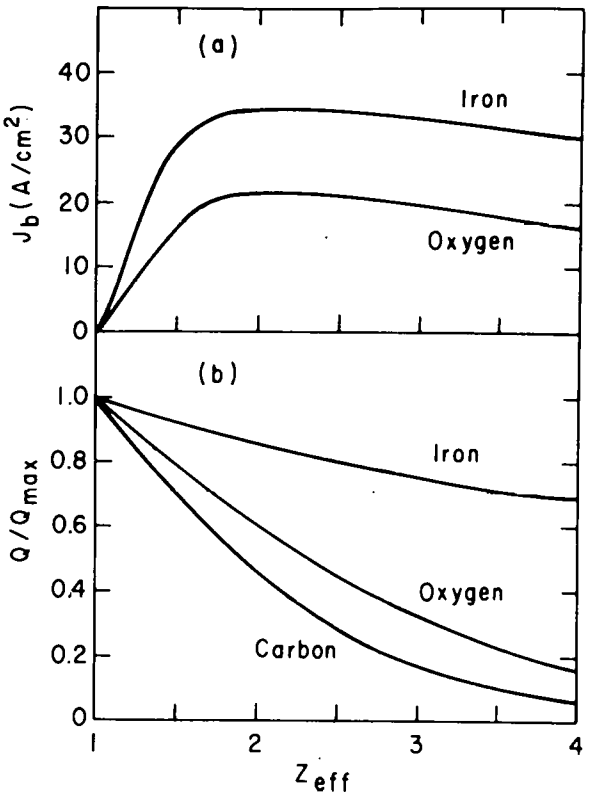

763780

FIG. 6. Effect of impurity ions on (a) beam-induced current and (b) Q. W_D = 60 keV, W_{T_3} = 90 keV. $P_{D°}$ = 0.67 W/cm^3; $P_{T°}$ adjusted to give $n_T = n_D$ when $\tau_p = \tau_{Ee}$. T_e = 6 keV. No charge exchange.

3. EQUILIBRIUM SIMULATION OF CIT PLASMAS

At the start of injection, the electric current of the energetic ions parallel to the magnetic field is cancelled identically by induced electron currents. These return currents relax with a very long time constant, equal to the bulk-plasma skin time. A guiding-center code, GUIDON [9], has been used to investigate the steady-state effects of unshielded injected-ion currents. In this spatially two-dimensional computer simulation, several thousand superparticles represent the fast ions. The guiding-center motions of the superparticles are followed in time and used to compute contributions to the toroidal current and plasma pressure profiles. The effects of electrons in the system are represented by an Ohmic current and by a drag force on fast ions.

The present calculations use W_D = 80 keV and W_T = 120 keV. A fast ion is removed from the system when its energy reaches 30 keV, or if it strikes a limiter at r = a; there are no warm ions. An ion that is removed is replaced immediately by a fast ion at full energy. The beam-induced current is calculated from the steady-state net toroidal momentum, using Eq. (1) with Z_{eff} = 1.5. In order to produce large J_b, one can set up by appropriate neutral-beam injection either (1) comparable but very large $n_T\langle v_{\parallel}\rangle_T$ and $n_D\langle v_{\parallel}\rangle_D$, or (2) a large $n_T\langle v_{\parallel}\rangle_T$ in the direction of the Ohmic current, and a relatively small $n_D\langle v_{\parallel}\rangle_D$ in the opposite direction. We find that method (2) is more suitable for obtaining a satisfactory equilibrium, because a large current set up by counterinjected ions tends to repel the other currents, resulting in excessive radial drift of the fast ions [9]. The flux-surface configuration is found to be well behaved if one produces $J_b \gtrsim J_{OH} \sim 75$ A/cm^2 with T° injection current about 1.5 times the D° injection current, giving $n_T/n_D \simeq 2$.

4. VELOCITY-SPACE STABILITY OF CIT PLASMAS

The ideal CIT system appears to have considerable free energy, because the ion velocity distribution is highly anisotropic ($p_{\parallel} \gtrsim 2p_{\perp}$), and $\partial f_h/\partial v_{\parallel}^2 > 0$ for $|v_{\parallel}| < u_b$, where u_b is the mean streaming velocity. Nevertheless, for all practical conditions the steady-state CIT velocity distributions are found to be stable to electrostatic and electromagnetic infinite-medium modes. This stability is due primarily to the large thermal spread of the ion distributions.

The ideal ion velocity distributions $f_h(v)$ (see Fig. 1) can be approximated by shifted Maxwellians with mean streaming velocity u_b, "temperature" $T_{h\parallel} \gtrsim 1.5\ T_e$ and $T_{h\perp} > T_{h\parallel}$. Other relations found from the FP results (see Table 1) are $v_{ti}/u_b > 1/3$ and $\Delta W/W_b > 4/3$, where $v_{ti} = (2T_{h\parallel}/M_h)^{1/2}$ and $\Delta W = 2\ u_b v_{ti} M_h$.

The stability of counterstreaming-ion distributions to electrostatic and electromagnetic velocity-space modes has been investigated in conjunction with both magnetospheric phenomena and laboratory experiments [10,11]. The stability criteria are summarized in Table 1. Since the streaming energy density can be treated formally as if it were a thermal pressure [12], the usual constraint on β_p for steady-state tokamak equilibrium (i.e., $\beta_p \lesssim R_o/a$) allows only a small value of u_b/v_{Alf}. The ideal $f_h(v)$ are apparently stable against all velocity-space modes, and practical $f_h(v)$ will be even more stable: That is, a substantial population of warm ions enhances the

TABLE I

Stability Criteria for Counterstreaming-Ion Velocity Distributions [10]

Mode	Sufficient Condition for Stability	CIT Parameters from FP Code
Electrostatic, ω not near ω_{ci}	$T_{\parallel} > 1/2\ T_e$, $u_b \lesssim 10(T_e/M_h)^{1/2}$	$T_{\parallel} \gtrsim 1.5\ T_e$ $u_b < 5(T_e/M_h)^{1/2}$
Electromagnetic, ω not near ω_{ci}	$u_b < 1/2\ v_{Alfven}$	$u_b \lesssim 1/5\ v_{Alfven}$
Electrostatic ion cyclotron waves	$\Delta W/W_b > 0.8\ T_e/T_\perp$	$\Delta W/W_b > 2\ T_e/T_\perp$
Electromagnetic ion cyclotron waves	$u_b < 1/3\ v_{Alfven}$ or $\Delta W/W_b \gtrsim 1$	$\Delta W/W_b > 4/3$

slowing-down rate of energetic ions, resulting in a smaller u_b, and also increases ΔW and $T_{h\parallel}$. In many practical cases, the total ion distribution — the sum of $f_h(v)$ for D^+ and T^+ — is single-humped, as in Fig. 4(b), and therefore is absolutely stable against velocity-space modes. Concerning MHD modes that could result from the anisotropic pressure, it is clear that the "firehose" instability cannot arise in tokamak operation, where $p_\parallel/B^2 \ll 1$.

5. FOKKER-PLANCK/RADIAL TRANSPORT CALCULATIONS

5.1 FPT Code

The Fokker-Planck code used to obtain the results of Sect. 2 has been combined with a one-dimensional transport code; the combined code is denoted FPT. The numerical techniques employed in FPT to solve the differential equations of plasma transport are described in detail elsewhere [13]. Here we summarize the plasma-physical treatment of the CIT problem as embodied in the code. In all cases steady-state solutions have been obtained, with excellent particle and energy conservation.

In FPT the particle and energy fluxes are calculated at 61 radial points, while FP calculations are performed at just 7 radial positions, with interpolations used at intermediate positions. The time step Δt for both the FP and transport calculations is 2 ms.

Transfer of Hot Ions to Warm Ions. Hot ions (injected by neutral beams) do not diffuse, but decelerate in place. The fundamental deceleration mechanism is Coulomb drag on electrons, so that upon reaching $W \simeq 3/2\ T_e$ a hot ion becomes part of the "warm-ion" population. It is most convenient in the FPT code to regard the warm-ion population as Maxwellian (and isotropic), and to transfer hot ions into this Maxwellian as follows: At each time-step, all hot ions with velocity in the range $0<v\leq v_{max}$, where

$$\int_0^{v_{max}} f_h(v)\ \frac{1}{2}\ M_h v^2 d\vec{v} = \frac{3}{8}\ T_i \int_0^{v_{max}} f_h(v) d\vec{v} \qquad (2)$$

are transferred. We justify this procedure a posteriori, since we find, generally, that $T_i/T_e = 2\text{-}3$. All warm-ion species (D^+, T^+, impurities) have the same temperature T_i — but usually have considerably different densities.

Transport Model. The dominant particle diffusion is that of warm ions; the electron density profile is determined by charge neutrality. Ions and electrons lose energy by particle convection and by thermal conduction. In the investigation reported here, the same diffusion constant D is employed for all particle and energy loss processes. Denoting a typical ion species by the subscript "a", a typical particle flux is

$$\Gamma_a = D\partial n_a/\partial r \quad . \qquad (3)$$

The ion heat flux is

$$Q_i = \frac{5}{4}\ D \sum_a \frac{\partial}{\partial r}\ (n_a T_i) \quad . \qquad (4)$$

The electron heat flux is

$$Q_e = \frac{5}{4} D \frac{\partial}{\partial r} (n_e T_e) \quad . \tag{5}$$

The diffusion constant is taken to be independent of all plasma parameters, and its magnitude is varied arbitrarily over the range observed in present tokamak experiments ($D \sim 3\times10^3$ to 3×10^4 cm^2/s) [1].

The electrons also lose energy by a bulk loss $3/2\ n_e T_e/\tau_r$, where $\tau_r(\text{sec}) = [0.1 + 0.3(1 - r/a)^{3/2}]$. This term simulates radiation loss, which dominates at the edge. The warm ions also lose energy by charge-exchange. The transport of neutral particles is not treated explicitly, but a stationary profile of neutral density is specified: $n_n(r)=n_n(0)\exp(k_n r/a)$. Hot ions that undergo charge exchange become warm ions at $3/2\ T_i$. Warm ions that undergo charge exchange lose all their energy.

Miscellaneous. (a) Electric fields are absent. Ohmic power dissipation is negligible for the conditions of interest. (b) Fusion alphas have been treated as a separate species but are not included here, since we find that their effect is only modest under conditions where $Q \sim 1$. (c) A source of cold ions (at zero energy) can be introduced according to a specified profile, $S_c(r)$.

5.2 Parameters for FPT Calculations.

The present study is concerned especially with finding plasma conditions for which $Q \geq 1$. The plasma dimensions are $R_o = 3.75$ m, $a = 0.75$ m (circular). For a number of practical reasons discussed elsewhere [4,14], the optimal W_b for CIT-type operation is 80 to 100 keV for D°. In this section we use $W_b = 80$ keV (D°) and 120 keV (T°).

Boundary Conditions. At the limiter radius ($r = a$), we fix $n_h = 0$, $n_e = n_i = 2.5\times10^{12}$ cm^{-3}, $T_e = T_i = 0.3$ keV. At $t = 0$, the density and temperature profiles are parabolic in radius, with $n_i(0) = 2\times10^{13}$ cm^{-3}, $n_{hot}(0) = 1\times10^{13}$ cm^{-3}, $T_e(0) = T_i(0) = 7.0$ keV. The hot-ion source current is parabolic in radius and constant in time, with $S_T = 0.75\ S_D$. Injection angles are $\theta_o = 0°$ for D° and 180° for T°, with beam width $\Delta\theta = 20°$.

Charge-Exchange. The neutral density at $r = 0$ is expected to be in the range $1\text{-}3\times10^7$ cm^{-3}. This population arises from (1) neutrals produced by charge-exchange trapping of injected neutrals [4]; (2) neutrals diffusing from outside the discharge (attenuated by several orders of magnitude). In a real plasma most of the neutrals from charge-exchanged fast ions would be recaptured in the plasma. Because we assume here that all hot neutrals are immediately lost from the plasma, we take $n_n(0) = 1\text{-}3\times10^6$ cm^{-3} as an effective range of values for use in the FPT code. The rate coefficient for charge exchange is taken to be 8×10^{-8} cm^3/s, independent of ion energy. The neutral density profile is $n_n(r) = n_n(0)\exp(5.7\ r/a)$, which gives $n_n(a)/n_n(0) = 300$.

5.3 Results of FPT Calculations

For a given set of parameters (P_{beam}, D, n_n, S_c) the evolution of the plasma conditions is followed until a steady state is attained. The time

to reach steady-state conditions is 0.6 to 1.2 s, which corresponds to approximately one "Spitzer slowing-down time." The profiles of n_e, n_i, n_{hot}, T_e and T_i differ somewhat from the parabolas chosen at t = 0, but are smoothly varying; at all positions one has $\partial n_a/\partial r$, $\partial T_i/\partial r$, $\partial T_e/\partial r < 0$. However, the average hot-ion energy $\langle W_h \rangle$ is sometimes peaked toward the outside, reflecting the strong charge-exchange loss rate in this region.

Figures 7 to 9 show the effects of plasma diffusion, charge-exchange loss, and cold-ion influx for conditions where $Q \gtrsim 0.8$. In all cases shown, P_{beam} is 170 MW, or 4.1 W/cm^3. (We find that Q increases with P_{beam}, other conditions being equal; the increase is due primarily to an increase in T_e. The 170 MW injection used here sometimes results in plasma densities that would be too high for acceptable beam penetration, and in plasma betas that are too large according to the usual MHD constraints. In practice, however, the plasma would be moderately elongated, thereby permitting a substantially higher beta. Reference [14] gives a practical example of a CIT-type fusion plasma with suitable MHD parameters and acceptable beam penetration.)

Effect of Warm-Plasma Diffusion Rate. Figure 7 shows the variation in key plasma parameters with $\langle n_e \rangle \tau_{Ee}$. In the steady state, an effective τ_{Ee} is calculated as the ratio of the total electron energy in the plasma to the sum of the rates of electron energy loss by diffusion to the limiter and by the bulk-loss process. To increase τ_{Ee} (and also τ_{Ei}), D is varied from 3×10^4 to 3×10^3 cm^2/s. At the smaller $n_e\tau_{Ee}$, the diffusion-loss rate for electron energy is comparable with the bulk-loss rate, whereas the warm-ion diffusion-loss rate greatly exceeds the charge-exchange loss rate (averaged over the entire plasma).

The following points are noteworthy: (1) With increasing $\langle n_e \rangle \tau_{Ee}$, the plasma evolves from the CIT regime with $n_{hot}/n_e \sim 1$ toward a TCT/thermonuclear regime where $n_{hot}/n_e \ll 1$ [7]. (2) While Q increases substantially at larger $\langle n_e \rangle \tau_{Ee}$, the accompanying large increase in n_e may prevent beam penetration. (3) Under most conditions one has $T_i/T_e \gtrsim 2$, which reflects the strong Coulomb coupling of the hot ions to the warm ions, as well as the deceleration of hot ions into the warm-ion distribution. In all cases $\Pi_i \gg 1$. (4) The average energy of the diffusing warm ions is substantial, namely $\langle 3/2\ T_i \rangle \sim 35$ keV. (5) With increasing warm-ion population, the hot ions decelerate more quickly, so that their charge-exchange loss is reduced. (6) Q is about 40% of the ideal CIT value [shown in Fig. 2(b)]. The reduction is due to the large charge-exchange loss of hot ions, and to the enhanced drag on warm ions.

Effect of Charge Exchange. Figure 8 shows the effect of increased neutral-density population. As discussed in Sect. 5.2, the values shown for $n_n\langle\sigma v\rangle_{cx}$ correspond to values 5 to 10 times higher in a real plasma of comparable $\langle n_e \rangle a$, where hot neutrals can be retrapped. For all conditions of Fig. 8, $\langle T_e \rangle$ = 10-11 keV. With increasing n_n, the hot-ion density suffers considerable depletion, and Q decreases markedly. T_i/T_e decreases with n_n because of increased charge-exchange loss of warm ions, but $\Pi_i \gg 1$ always.

Effect of Cold-Ion Influx. Ionization of neutrals entering the plasma results in a source of cold ions. In addition cold plasma from the "scrape-off region" can enter the discharge. Figure 9 shows the effect of substantial F_c = cold-ion influx/hot-ion influx, using the cold-ion source profile $S_c(r) = S_c(0)[1-r/a]\exp(6.0\ r/a)$.

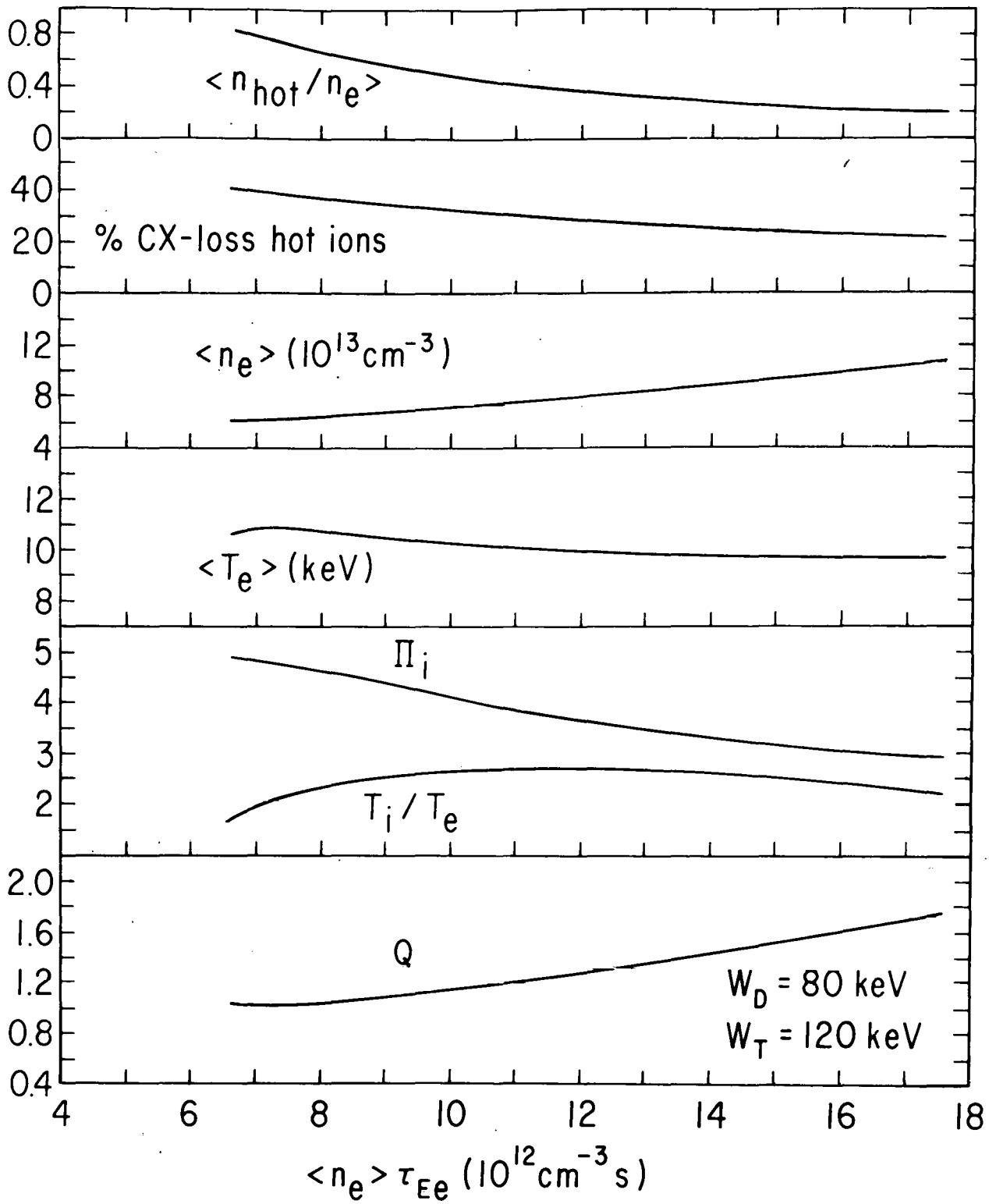

763823

FIG. 7. FPT calculations for CIT performance as a function of $\langle n_e \rangle \tau_{Ee}$ determined from diffusion and bulk losses. Parameters are averaged over entire plasma (a = 75 cm). T_i is warm-ion temperature. Effective $n_n \langle \sigma v \rangle_{cx}$ - 0.1 s^{-1} at r = 0, 30 s^{-1} at r = a. 17.6 MeV per reaction.

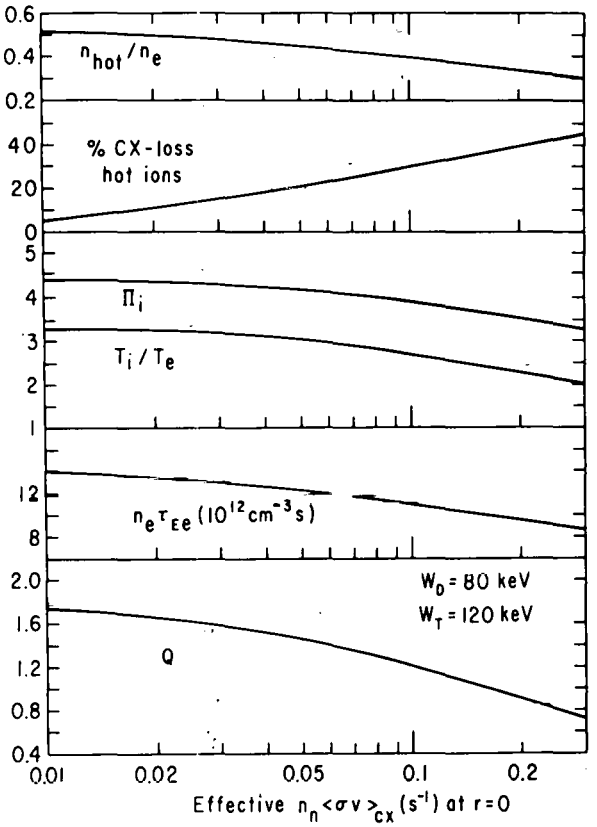

763781

FIG. 8. FPT calculations for CIT performance as a function of effective charge-exchange rate at r = 0. (Hot neutrals are not retrapped.) $n_n(r) = n_n(0)\exp(5.7\ r/a)$. T_i is warm-ion temperature. D = 6×10^3 cm^2/s.

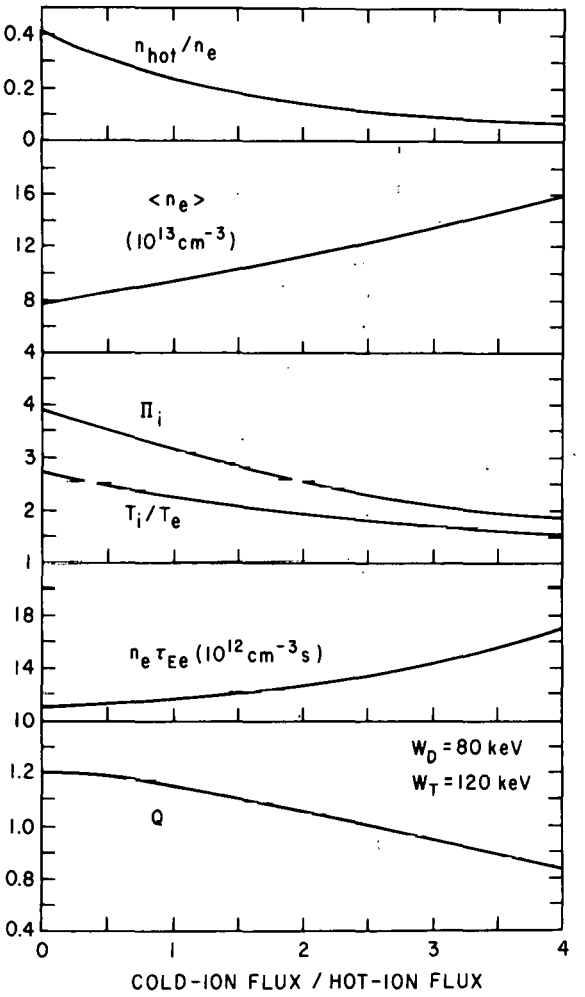

763782

FIG. 9. FPT calculations for CIT performance as a function of relative cold-ion flux. Hot-ion flux is total beam injection rate (1.1×10^{22} particles/s). T_i is warm-ion temperature. Effective $n_n\langle\sigma v\rangle_{cx}$ = 0.1 s^{-1} at r = 0, 30 s^{-1} at r = a. D = 6×10^3 cm^2/s.

For $F_c >> 1$, n_{hot}/n_e becomes very small, indicating that the plasma has entered the TCT regime where the beams supply only a fraction of the plasma fueling, and beam-target fusion reactions are dominant. Both T_e and T_i/T_e decrease markedly, but one still has $T_i/T_e \gtrsim 3/2$. In the transition to this low-T_e TCT regime, Q drops by 30% while $n_e\tau_{Ee}$ increases by 55%. Again, the factor of 2 increase in n_e would make beam penetration difficult. These results illustrate that to obtain $Q \simeq 1$ at smaller $n_e\tau_{Ee}$ with acceptable beam penetration, it is important to provide a means of rapid particle exhaust from the torus [7] — such as an "unload" magnetic divertor.

6. RELEVANCE OF PRESENT EXPERIMENTS

Start-up. In the 2XIIB mirror machine, build-up of high plasma density is achieved by neutral-beam injection on a warm low-density target plasma [15] in a manner analogous to that proposed for CIT start-up (see Sect. 2.1). In the 2XIIB plasma, $n_{hot}/n_e = 0.85$.

Plasma Recycling. Optimal CIT operation places severe limits on the allowed influx of cold plasma and neutrals into the reacting region. By special discharge-cleaning techniques, very low recycling has been obtained in the Alcator and Microtor devices [16], where the density drops continuously in time unless puffs of gas are injected into the plasma. In the ATC device, the same result has been achieved by titanium gettering of the vacuum wall [17]. Two new divertor experiments, DITE and PDX, can be operated with "unload" divertors that should rapidly exhaust ions that diffuse out of the discharge.

$\Pi_i >> 1$. In TFR, ORMAK, and ATC [1], high-powered beam injection has produced $\langle T_i \rangle \gtrsim \langle T_e \rangle$, so that the large bulk-ion temperature is sustained wholly by the injected beams. The total energy of the warm ions and energetic ions exceeds the electron energy by as much as 50%: i.e., $\Pi_i \simeq 1.5$. In the new DITE, PLT, and PDX devices, W_b will be sufficiently low so that at least half the beam energy will be transferred to bulk-plasma ions, and the beams themselves will provide significant fueling. Therefore, one expects a continuation of the present experimental trend toward $\Pi_i >> 1$ and $T_i > T_e$ — the realm of energetic-ion plasmas.

---

*Work supported by U. S. Energy Research and Development Administration Contracts E(11-1)-3073 and W-7405-ENG-48.

REFERENCES

[1] ORMAK Group, Paper IAEA-CN-35/A4-1, these Proceedings; TFR Group, Paper IAEA-CN-35/A4-2, these Proceedings; ELLIS, R. A., EUBANK, H. P., GOLDSTON, R. J., SMITH, R. R., NAGASHIMA, T., Nucl. Fusion 16 (1976) 524.

[2] KULSRUD, R. M., JASSBY, D. L., Nature 259 (1976) 541.

[3] CORDEY, J. G., CORE, W. G. F., Nucl. Fusion 15 (1975) 710.

[4] JASSBY, D. L., Nucl. Fusion 16 (1976) 15.

[5] CORDEY, J. G., HAAS, F. A., Culham Lab. Rep. CLM-P448 (1976).

[6] KILLEEN, J., MIRIN, A. A., RENSINK, M. E., Methods in Computational Physics (Academic Press, New York, 1976) Vol. 16, Ch. XI.

[7] JASSBY, D. L., TOWNER, H. H., Princeton Plasma Physics Lab. Rep. MATT-1180 (1976).

[8] OHKAWA, T., Nucl. Fusion 10 (1970) 185.

[9] JOHNSON, T. H., KILLEEN, J., ANDERSON, O. A., RENSINK, M. E., "Guiding-Center Simulation of Toroidal Plasmas," Lawrence Livermore Lab. Rep. UCRL-78597 (1976), to be published in J. Comput. Physics.

[10] JASSBY, D. L., KULSRUD, R. M., PERKINS. F. W., "Velocity-Space Stability of Counterstreaming-Ion Tokamak Plasmas," Princeton Plasma Physics Lab. Rep. MATT-1233 (1976) and references therein.

[11] PERKINS, F. W., Phys. Fluids 19 (1976) 1012.

[12] BOOZER, A. H., BERK, H. L., private communications (1976).

[13] MIRIN, A. A., KILLEEN, J., MARX, K. D., RENSINK, M. E., "A Radial Transport/Fokker-Planck Model for a Tokamak Plasma," Lawrence Livermore Lab. Rep. UCRL-76770 (1976), to be published in J. Comput. Physics.

[14] JASSBY, D. L., LEE, J. D., "Counterstreaming-Ion-Tokamak Fissile Breeder," Proc. US-USSR Symposium on Fusion-Fission Reactors (Lawrence Livermore Lab., 1976).

[15] COENSGEN, F. H., et al., Phys. Rev. Lett. 37 (1976) 143.

[16] ALCATOR Group, Paper IAEA-CN-35/A5, these Proceedings; TAYLOR, R. J., private communication (1976).

[17] STOTT, P. E., DAUGHNEY, C. C., ELLIS, R. A., Nucl. Fusion 15 (1975) 431.